Water Research 184 (2020) 116144

Contents lists available at ScienceDirect

Water Research

journal homepage: www.elsevier.com/locate/watres

Identification of primary effecters of N_2O emissions from full-scale biological nitrogen removal systems using random forest approach

Min Joon Song [a], Sangki Choi [b], Wo Bin Bae [b], Jaejin Lee [c], Heejoo Han [a], Daehyun D. Kim [a], Miye Kwon [a], Jaewook Myung [a], Young Mo Kim [d], Sukhwan Yoon [a, *]

[a] Department of Civil and Environmental Engineering, KAIST, Daejeon, 34141, Republic of Korea
[b] School of Earth Sciences and Environmental Engineering, Gwangju Institute of Science and Technology, Gwangju, 61005, Republic of Korea
[c] Department of Agricultural and Biosystems Engineering, Iowa State University, Ames, IA, 50011, United states
[d] Department of Civil and Environmental Engineering, Hanyang University, Seongdong-gu, Seoul, 04763, Republic of Korea

ARTICLE INFO

Article history:
Received 18 March 2020
Received in revised form
30 June 2020
Accepted 2 July 2020
Available online 6 July 2020

Keywords:
Nitrous oxide
Wastewater treatment plants
Biological nitrogen removal
Nitrification
Denitrification
Random forest

ABSTRACT

Wastewater treatment plants (WWTPs) have long been recognized as point sources of N_2O, a potent greenhouse gas and ozone-depleting agent. Multiple mechanisms, both biotic and abiotic, have been suggested to be responsible for N_2O production from WWTPs, with basis on extrapolation from laboratory results and statistical analyses of metadata collected from operational full-scale plants. In this study, random forest (RF) analysis, a machine-learning approach for feature selection from highly multivariate datasets, was adopted to investigate N_2O production mechanism in activated sludge tanks of WWTPs from a novel perspective. Standardized measurements of N_2O effluxes coupled with exhaustive metadata collection were performed at activated sludge tanks of three biological nitrogen removal WWTPs at different times of the year. The multivariate datasets were used as inputs for RF analyses. Computation of the permutation variable importance measures returned biomass-normalized dissolved inorganic carbon concentration ($DIC \cdot VSS^{-1}$) and specific ammonia oxidation activity ($sOUR_{AOB}$) as the most influential parameters determining N_2O emissions from the aerated zones (or phases) of activated sludge bioreactors. For the anoxic tanks, dissolved-organic-carbon-to-NO_2^-/NO_3^- ratio ($DOC \cdot (NO_2^-N + NO_3^-N)^{-1}$) was singled out as the most influential. These data analysis results clearly indicate disparate mechanisms for N_2O generation in the oxic and anoxic activated sludge bioreactors, and provide evidences against significant contributions of N_2O carryover across different zones or phases or niche-specific microbial reactions, with aerobic NH_3/NH_4^+ oxidation to NO_2^- and anoxic denitrification predominantly responsible from aerated and anoxic zones or phases of activated sludge bioreactors, respectively.

1. Introduction

Nitrous oxide (N_2O) has recently attracted immense scientific interest amid the escalating concern for global warming and climate change. The global contribution of N_2O to the net greenhouse gas emissions is relatively minor (~6% in terms of CO_2eq) as compared to those of CO_2 (~76%) and CH_4 (~16%). Developing strategies for mitigating N_2O emissions is nevertheless crucial for curbing climate change, given its high global warming potential, ~300 times greater than that of CO_2 in a 100-year scale (IPCC , 2014).

The contribution of the wastewater treatment sector to the net anthropogenic N_2O emissions used to be regarded insignificant at ~3.5%. With the recent upward adjustment of the emission factor from 0.00035 to 0.016 kg N_2O–N/kg TN load, however, WWTPs would now be one of the most potent N_2O sources (IPCC et al., 2014; 2019). Further, a steady increase in water usage is projected in the foreseeable future, which would lead to further growth in global N_2O emissions from the wastewater treatment sector (Flörke et al., 2013). Recently, WWTPs are increasingly viewed as water resource recovery facilities (WRRFs) (Lam et al., 2020). Coping with N_2O emissions would undoubtedly be crucial for the transition of current WWTPs to carbon-neutral WRRFs, as N_2O is often considered as the largest contributor to life-cycle greenhouse gas emissions from WWTPs (Vasilaki et al., 2019).

* Corresponding author.
E-mail address: syoon80@kaist.ac.kr (S. Yoon).

https://doi.org/10.1016/j.watres.2020.116144
0043-1354/

Despite decades of investigation, the N_2O-producing mechanisms in biological nitrogen removal (BNR) wastewater treatment plants (WWTPs) are not yet fully understood. In the conventional BNR systems, where NH_4^+-N is removed via nitrification (NH_3/NH_4^+-to-NO_3^- oxidation via NO_2^-) and denitrification (NO_3^--to-N_2 reduction via NO_2^-, NO, and N_2O), >90% of N_2O production originates from bioreactors where these N-dissimilation reactions take place (Kampschreur et al., 2009). Ammonia-oxidizing bacteria (AOB) and heterotrophic denitrifying bacteria are the microbial guilds deemed majorly responsible for N_2O production from nitrification and denitrification, respectively (Kampschreur et al., 2009). Several hypotheses regarding conditions leading to increased N_2O production from these microbial guilds have been suggested based on *in vitro* observations. High pH, low dissolved oxygen (DO) concentration, high NH_4^+ and NO_2^- concentrations, and dissolved inorganic carbon (DIC) excess or deficiency have been suggested to increase N_2O formation from ammonia oxidation, and low C:N (or COD/N) ratio, low pH, O_2 intrusion, and high NO_2^- concentration have been hypothesized to increase N_2O release from incomplete denitrification (Itokawa et al., 2001; Pan et al., 2012; Peng et al., 2014; Peng et al., 2015a; b; Wunderlin et al., 2012). Whether N_2O emissions from BNR bioreactors are actually affected by these conditions, however, has not been sufficiently supported with datasets collected from full-scale operational WWTPs (Kosonen et al., 2016; Rodríguez-Caballero et al., 2015).

Over decades, several researchers have attempted to statistically identify the effecters with greatest influence on N_2O emissions from AS bioreactors (Aboobakar et al., 2013; Ahn et al., 2010; Vasilaki et al., 2018). Considering the practical difficulty of N_2O flux measurements *in situ* and the large numbers of parameters characterizing the AS operations in WWTPs, limited sample size (n) and high dimensionality were the defining characters of the datasets used as inputs for these statistical analyses. The multiple regression approach and feature extraction approach taken in these previous analyses may not have been the optimal methodological approaches given the circumstances. Multiple regression fitting too many effecters to a single outcome may often result in noisy and even arbitrary interpretations due mainly to the curse of dimensionality, especially when the number of features far exceeds the sample size (Hastie et al., 2005; Krzywinski and Altman, 2015). Expansion of the datasets by compiling previously published N_2O emissions data can easily be considered an option as the solution to this dilemma. Although no shortage of on-site N_2O emission monitoring campaigns have been conducted at pilot- and full-scale WWTPs across the globe, inconsistent monitoring strategies have been adopted for these campaigns (Ahn et al., 2010; Daelman et al., 2015; Kampschreur et al., 2009; Kosonen et al., 2016). The Environmental Protection Agency (EPA)-certified standard method for N_2O flux measurement has been established only as late as 2011 (Chandran, 2011). Even after its stipulation, N_2O emission data have continued to be collected with nonuniform methodologies that have not been cross-validated (Ni et al., 2013; Vieira et al., 2019). Further, the categories of metadata collected with the N_2O flux measurements are often inconsistent across these previous studies (Ahn et al., 2010; Vasilaki et al., 2018). Due to these reasons, amassing of existing datasets from the literature would not be the cure for curse of dimensionality. Principle component analysis (PCA) using a feature extraction approach has been adopted as an alternative statistical method to circumvent the high dimensionality dilemma by reducing the dimensions of the original features. The loss of intrinsic semantics of original features and susceptibility to misapplication, often leading to potential misinterpretation of the outputs, however, can be problematic with this approach (Lever et al., 2017; Tang et al., 2014).

In this study, random forest (RF) analysis was applied to associate the N_2O emissions data to the WWTP metadata to approach the endeavor from a novel perspective. This statistical method takes an embedded feature selection approach that has proven effective in analyzing datasets with limited number of data points and high dimensionality without sacrificing information embedded in the original features (Breiman, 2001; Tang et al., 2014). Random forest has proven effective in exploratory data analyses, as (1) removal of irrelevant and/or redundant features allows for improved comprehensibility (2) no assumption regarding the quality of data (e.g., normality and linearity), needs to be satisfied, and (3) it is less sensitive to tampering of the hyperparameters and thus, resistant to intentional or unintentional overfitting (Breiman, 2001; Statnikov et al., 2008; Vincenzi et al., 2011). Further, RF analysis is especially convenient in narrowing down features according to their relative influences to the outcome, as RF returns variable importance measures (VIM) for each input feature (Gregorutti et al., 2017). Random Forest analysis has been implemented in diverse disciplines of science, including, for example, clinical sciences, where genes most relevant to certain clinical outcomes were selected for more efficient analyses of microarray data, and ecological sciences, where environmental parameters associated with certain ecological phenomena were ranked according to their relative importance (Díaz-Uriarte and Alvarez de Andrés, 2006; Hollister et al., 2016; Vincenzi et al., 2011). The datasets as inputs for the RF analyses were collected using uniform standardized methods from AS tanks at three full-scale WWTPs with different configurations and operating conditions over a 10-month period from April 2018 to January 2019. The collected datasets were then utilized to compute the variable importance measures (VIM) of the AS parameters, i.e., the statistic indicators used for selection of the most influential parameters (Breiman, 2001).

2. Materials and methods

2.1. Description of the full-scale wastewater treatment plants

The monitoring campaign was carried out at three WWTPs located near Gwangju, South Korea over a 10-month span from April 2018 to January 2019. The names and the exact locations of the WWTPs will not be disclosed due to confidentiality issues, and the WWTPs will be referred to as plants A, B, and C instead (Fig. 1, Table 1). The plant A is a conventional 8-train A2O (anaerobic-anoxic-oxic) WWTP with the return activated sludge (RAS) rate of 1,300 $m^3\ h^{-1}\cdot train^{-1}$. Only one of the eight trains was monitored in the campaign. The plant B is an AO (anoxic-oxic) membrane bioreactor (MBR) that utilizes the membrane modules in the oxic tank to sustain high solids retention time (SRT) without RAS. Overflow from the oxic tank returns the AS to the anoxic tank, where denitrification takes place. The effluent is partially reused for in-facility and gardening purposes. The plant C is a four-step (fill − aeration − sedimentation − draw) sequencing batch reactor (SBR) with 2.37 h as the duration of each complete cycle. At each cycle, 250 m^3 of 2,250 m^3 mixed liquor in the bioreactor tank is withdrawn at the draw step and refilled with influent wastewater at the fill step of the following cycle. Heterotrophic denitrification takes place during the fill step, removing NO_3^- generated from nitrification of NH_4^+ in the oxic steps (the aeration and sedimentation steps) of the preceding cycle. No organic carbon supplement is added at any of the three WWTPs. Detailed operating parameters of the three WWTPs are presented in Table 1.

2.2. Measurement of N_2O emissions from the WWTPs

The N_2O fluxes from the AS bioreactors were measured using a

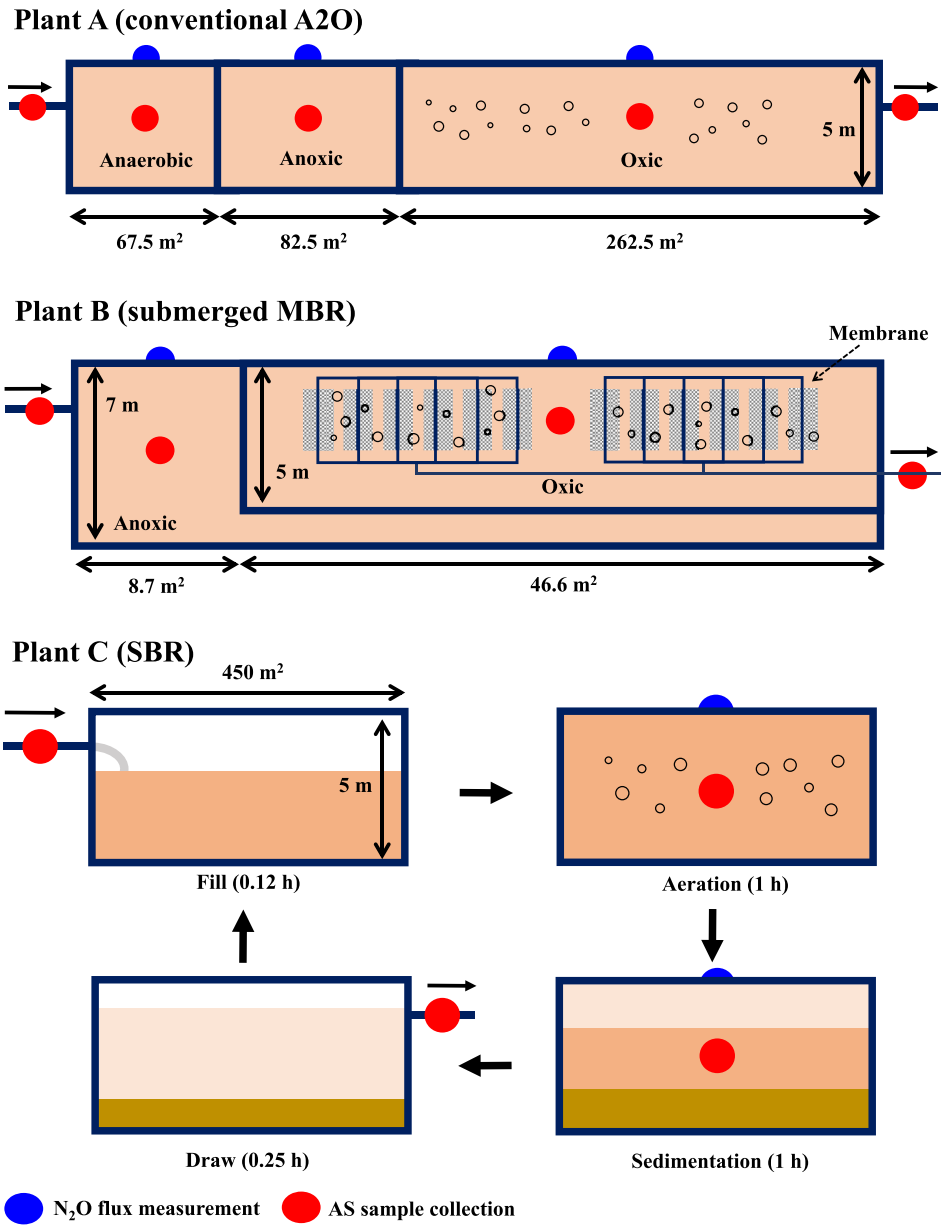

Fig. 1. The schematic diagrams depicting the biological treatment processes of the three WWTPs examined in this study.

floating flux chamber constructed according to the specification in the US EPA guideline (Chandran, 2011). The main body of the flux chamber was constructed with aluminum and glued to a rubber tire for flotation (the schematic diagram presented in Fig. S1). One of the five gas ports fitted on the aluminum dome was connected via PFA Teflon™ tubing to a Teledyne T320E infrared gas analyzer (San Diego, CA) for on-line measurement of N_2O in effluent gas. A gas port was used for streaming the tracer gas (10% v/v He in N_2; all gases were supplied by Daeduk Gas Co. Daejeon, Korea) through the chamber, and another port for supply of carrier gas (>99.999% N_2) to meet the minimum flowrate for the gas analyzer when measuring N_2O flux from quiescent bioreactors. Before each measurement, two-point calibration was performed using >99.999% N_2 gas and N_2 gas carrying 100 ppmv N_2O. The floating flux chamber was positioned at the geometric center of each bioreactor zone, where the measured N_2O flux would best represent the average flux from the zone (Chandran, 2011). Tracer gas was passed through the chamber at a flowrate of 1 L min^{-1} and the He concentration in the effluent gas was measured with a HP-5890 gas chromatograph equipped with a thermal conductivity detector and Porapak Q column (Agilent Technologies, Palo Alto, CA). For N_2O flux measurements at the aerated zones or phases of AS bioreactors, N_2O and He concentrations in the off-gases exiting through the flux chamber were measured without aid of external carrier gas. For measurements of N_2O flux from quiescent tanks, high-purity N_2 sweep gas was blown into the headspace of the flux chamber at a constant flowrate of 5 L min^{-1}, and the N_2O and He concentrations in the effluent sweep gas were measured. For the plants A and B, the N_2O flux was monitored for 30 min at each zone with different aeration regime. The gas flowrates from the chambers placed on the aerated and quiescent zones or phases were calculated using Equations (1) and (2), respectively (Chandran, 2011).

Table 1
Description of the BNR processes at the examined WWTPs.

Plant	A (A2O)	B (MBR)	C (SBR)	Unit
Tank volume per train	Total: 2,064 Anaerobic: 338 Anoxic: 413 Oxic (aerated): 1313	Total: 387 Anoxic: 154 Oxic (aerated): 233	Total: 2,250	m^3
Number of trains	8	2	2	–
External return activated sludge	1,300	–	–	$m^3 \cdot h^{-1}$
Internal return activated sludge	370	250	–	$m^3 \cdot h^{-1}$
Design HRT	Total: 6.7 Anaerobic: 1.1 Anoxic: 1.3 Oxic: 4.2	Total: 8.0 Anoxic: 3.2 Oxic: 4.8	Total: 2.37 Fill: 0.12 Aeration: 1 Sedimentation: 1 Draw: 0.25	h
Actual HRT	Total: 7.4 Anaerobic: 1.2 Anoxic: 1.5 Oxic: 4.7	Total: 15.3 Anoxic: 6.1 Oxic: 9.2	Operates at design HRT	h
Design SRT	12.1	30	20	d
Actual SRT	7.6	20.6	22.5	d
Aeration rate at the oxic zone/phase	27,200	86,400	56,600	$m^3 \cdot d^{-1}$
Treatment capacity	60,000	16,000	4,500	$m^3 \cdot d^{-1}$

$$Q_e = \frac{Q_{tracer} \times (C_{He-tracer} - C_{He-fc})}{C_{He-fc}} \quad (1)$$

$$Q_e = \frac{Q_{tracer} \times (C_{He-tracer} - C_{He-fc})}{C_{He-fc}} - Q_{sweep} \quad (2)$$

where Q_e is the flowrate of the gas exiting the chamber ($L^3 \cdot T^{-1}$); Q_{tracer} is the flowrate of the tracer gas introduced into the chamber ($L^3 \cdot T^{-1}$); $C_{He\text{-}tracer}$ and $C_{He\text{-}fc}$ are the concentrations of He in the influent stream of the tracer gas and the effluent stream from the flux chamber, respectively ($M \cdot L^{-3}$); and Q_{sweep} is the flowrate of the sweep gas introduced into the chamber ($L^3 \cdot T^{-1}$).

The N_2O concentration in the effluent gas from the chamber was recorded every minute and the average of the concentrations was taken as the representative value. As the plant C is an SBR with the N_2O emission profile changing over time within each step, a slightly different approach was taken for N_2O flux measurement. At the aeration and sedimentation steps, the N_2O concentration in the chamber effluent was monitored over the entire step (e.g., for the entire hour of the aeration step) and the concentrations were averaged for calculation of the representative N_2O flux value. Due to technical difficulty, N_2O monitoring was not possible during the fill and draw steps. The on-line N_2O measurements were intermittently cross-checked with the N_2O concentrations measured with HP6890 Series gas chromatograph equipped with an electron capture detector (Agilent, Palo Alto, CA, USA). The N_2O flux was calculated using Equation (3).

$$J_{N2O} = \frac{Q_e \times C_{N2O}}{A_c} \quad (3)$$

where, J_{N2O} is the N_2O flux ($M \cdot L^{-2} \cdot T^{-1}$); C_{N2O} is the representative effluent N_2O concentration ($M \cdot L^{-3}$); and A_c is the water surface area covered by the flux chamber (L^2).

2.3. Determination of the specific ammonia oxidation activity of activated sludge samples

The AOB-specific oxygen uptake rate ($sOUR_{AOB}$) was measured using a batch respirometric assay as an estimate of the NH_3 oxidation activity of an oxic AS sample (Chandran and Smets, 2005). The culture medium contained per liter, 500 mg $KHCO_3$, 27.2 mg KH_2PO_4, 300 mg $MgSO_4 \cdot 7H_2O$, 180 mg $CaCl_2 \cdot 2H_2O$, and 1 mL each of the trace element solutions I and II (van de Graaf et al., 1996). Two sets of triplicate reaction vessels were prepared per sample, with 30-mL culture medium distributed to 40-mL Plexiglass respirometry chambers (Unisense, Aarhus, Denmark). The respirometric assays performed with the triplicate vessels amended with 5 mg $NH_4^+ \cdot L^{-1}$ estimated the $sOUR_{AOB+NOB+HET}$ value, i.e., the sum of sOURs owing to respiration of AOB, NOB (nitrite-oxidizing bacteria), and heterotrophs. The other set of triplicate vessels amended with 5 mg $NO_2^- \cdot L^{-1}$ was used to estimate the $sOUR_{NOB+HET}$ value. The vessels were vigorously bubbled with compressed air prior to addition of the AS biomass. The assays were performed on site with the AS samples collected during the N_2O flux measurements at the aerated zones or phases. The pellets collected from centrifugation of 30-mL samples were washed with 2 mM phosphate buffer solution (pH 7.0) and resuspended in 2 mL buffer solution. A 0.5-mL aliquot of the suspension was added to each of the triplicate respirometry chambers carrying aerated medium. The decrease in the DO (dissolved oxygen) concentration was monitored with a MicroRespiration system equipped with an OX-MR microelectrode (Unisense). For computation of the sOUR value, the maximum observed linear oxygen consumption rate within the first 30 min of incubation was normalized with the biomass calculated from the volatile suspended solids (VSS) concentration. The $sOUR_{AOB}$ value was obtained by subtracting $sOUR_{NOB+HET}$ from $sOUR_{AOB+NOB+HET}$. No oxygen consumption was observed in the abiotic controls prepared identically but incubated without addition of AS biomass. All measurements were performed in triplicates and the average values were taken for further analysis. The standard deviations of the $sOUR_{AOB}$ values were calculated with the propagation of error method.

2.4. Physico-chemical characterization of collected wastewater samples

The water temperature, pH, and DO concentration of AS were measured with an Orion Star™ A329 portable multiparameter meter (Thermo Scientific, Waltham, MA) immediately before each N_2O flux measurement. Simultaneously, AS samples were collected and 100-mL subsamples were passed through 0.2-μm filters (Advantec, Inc., Tokyo, Japan). The filtrates were stored at −20 °C

until further analyses. The total dissolved carbon (TDC), total dissolved organic carbon (DOC), and total dissolved nitrogen (TN) concentrations were determined using a Vario TOC cube (Elementar Analysensysteme GmbH, Langenselbold, Germany). The total dissolved inorganic carbon (DIC) concentration was calculated by subtracting the DOC concentration from the TDC concentration. The volatile suspended solids (VSS) concentration was determined by subtracting the solid mass measured after 2-h incineration at 550 °C from the initial suspended solid mass (APHA, 2017). The NH_4^+-N, NO_2^--N, and NO_3^--N concentrations were measured using a 930 Compact IC Flex ion chromatograph (Metrohm, Herisau, Switzerland) equipped with a Metrosep A Supp 5 anion exchange column and a Metrosep C4 cation exchange column. All measurements were performed in duplicates, and their averages were used for further analyses.

2.5. Feature selection with random forest analysis

The random forest (RF) method was used for feature selection from the collected datasets. The RF algorithm is an ensemble-learning algorithm, in which the final prediction is reached from the majority voting of the decisions made with multiple decision trees constructed with randomly permuted features and observations via recursive partitioning (Breiman, 2001). The data collected from the WWTP monitoring campaigns (Tables S2–S4) were subdivided into in-bag samples utilized as training sets (15 and 10 samples for aerated and anoxic AS, respectively) for growing the 'random forest' and out-of-bag (OoB) samples as test sets for evaluating the prediction performance (5 and 3 samples for aerated and anoxic AS, respectively). The random permutations of the in-bag observations and features were used to grow the forest, creating multiple decision trees with weakened intrinsic association between the observations and the features in the original dataset. The nodes of each individual tree were hierarchically structured to minimize the Gini impurity, i.e., maximize the information gain, at each bifurcation (Equation (4)) (Breiman, 2001).

$$I_G = 1 - f_1^2 - f_2^2 \tag{4}$$

where I_G is the gini index for a binary split and f_i is the proportion of the samples classified as the ith group at the node.

Individual features were ranked according to their variable importance measures (VIM) (Strobl et al., 2007). The VIM value of each feature was computed following its permutation in each of the trees in the random forest (Equation (5)) (Janitza et al., 2013).

$$VIM(X_j) = \frac{1}{n_{tree}} \sum_{t=1}^{n_{tree}} [E_t(X_j) - E_t] \tag{5}$$

where, VIM(X_j) is the variable importance measure of the feature X_j, n_{tree} is the number of trees in the forest, E_t and $E_t(X_j)$ are the misclassification rates of the tree t before and after permuting X_j, respectively, as tested with the OoB bag samples.

The RF classification was performed using the *randomForest* function of the randomForest package in RStudio v. 1.2.5 (Liaw and Wiener, 2012). For binary classification, the response variable (N_2O flux) was discretized to categorical attributes with the threshold set to the median value (303 and 163 mg N_2O–N·$m^{-2}d^{-1}$ for aerated and anoxic zones or phases, respectively), such that the outcome of the RF prediction can be classified as either 'high' or 'low' N_2O emission. The variables for construction of individual trees were randomly selected by bootstrapping with replacement. The hyperparameters were set as follows: ntree = 500, mtry = default (the square root of the number of variables), metric = accuracy, and importance = true. The classification performance was evaluated with the accuracy (Equation (6)), sensitivity (Equation (7)), and specificity (Equation (8)) presented in a confusion matrix (Powers, 2011). The VIM values were computed using the function *varimp* with the scale and type parameters set to false and 1, respectively.

$$Accuracy = \frac{\#\ of\ correct\ predictions\ (TH + TL)}{Total\ \#\ of\ predictions\ (TH + TL + FH + FL)} \tag{6}$$

$$Sensitivity = \frac{\#\ correctly\ predicted\ as'high'\ (TH)}{Total\ \#\ predicted\ as'high'(TH + FL)} \tag{7}$$

$$Specificity = \frac{\#\ correctly\ predicted\ as''low''\ (TL)}{Total\ \#\ predicted\ as'low'\ (TL + FH)} \tag{8}$$

where, TH, TL, FH, and FL stand for true high, true low, false high, and false low, respectively.

2.6. Statistical tests and correlation analyses

All statistical analyses were performed using RStudio v. 1.2.5 (RStudio Team, 2015). Given that only a few of the AS parameters fully satisfied the assumptions for parametric statistical tests (e.g., normality and homoscedasticity), all statistical tests were performed using non-parametric statistical tests. Statistical significances of pairwise comparisons were determined with the Mann-Whitney test (Fay and Proschan, 2010). The Kruskal-Wallis test was used when three measurements were compared (Kruskal and Wallis, 1952). Bivariate associations between the AS parameters were evaluated using tie-corrected Spearman tests (Dodge, 2008).

3. Results and discussion

3.1. Long-term monitoring of BNR WWTP performances and N_2O emissions

Twenty sets of data including the operating parameters, AS characteristics, and N_2O flux records were collected from the three WWTPs during the monitoring period (Tables S1–S4). The dissolved organic carbon (DOC) and total nitrogen (TN) removal performances were inconsistent, with the removal efficiencies ranging between 7.8-57.9% and 17.0–95.5%, respectively. As with the removal efficiencies, many of the operating parameters and AS characteristics critical for proper functioning of the BNR systems exhibited large temporal fluctuations, as well as variations across the WWTPs. The DO, DOC, DIC, TN, NH_4^+-N, and NO_3^--N concentrations in all examined AS bioreactors exhibited temporal fluctuations amounting to percent relative ranges larger than 150% over the ten-month span of the monitoring campaign. The only parameter with statistically significant difference across the WWTPs was the VSS concentration. Activated sludge sampled from the aerated zone of plant B had significantly higher ($p = 0.00$) VSS concentration (7050 ± 1320 mg VSS·L^{-1}) than aerated AS from the plants A (1660 ± 250 mg VSS·L^{-1}) and C (2110 ± 216 mg VSS·L^{-1}). The anoxic zone of the plant B (3020 ± 1010 mg VSS·L^{-1}) also had significantly higher VSS concentrations ($p = 0.03$) than the anoxic zone of the plant A (1260 ± 500 mg VSS·L^{-1}). The prolonged monitoring period enabled incorporation of temperature as an independent variable in the statistical analyses, as the water temperature varied between ~15 and ~30 °C at the WWTPs during the period.

The N_2O flux data were collected from the AS bioreactors of the BNR systems (Fig. 2). The three BNR systems exhibited substantially different N_2O emission profiles. At the full-scale A2O plant (plant A)

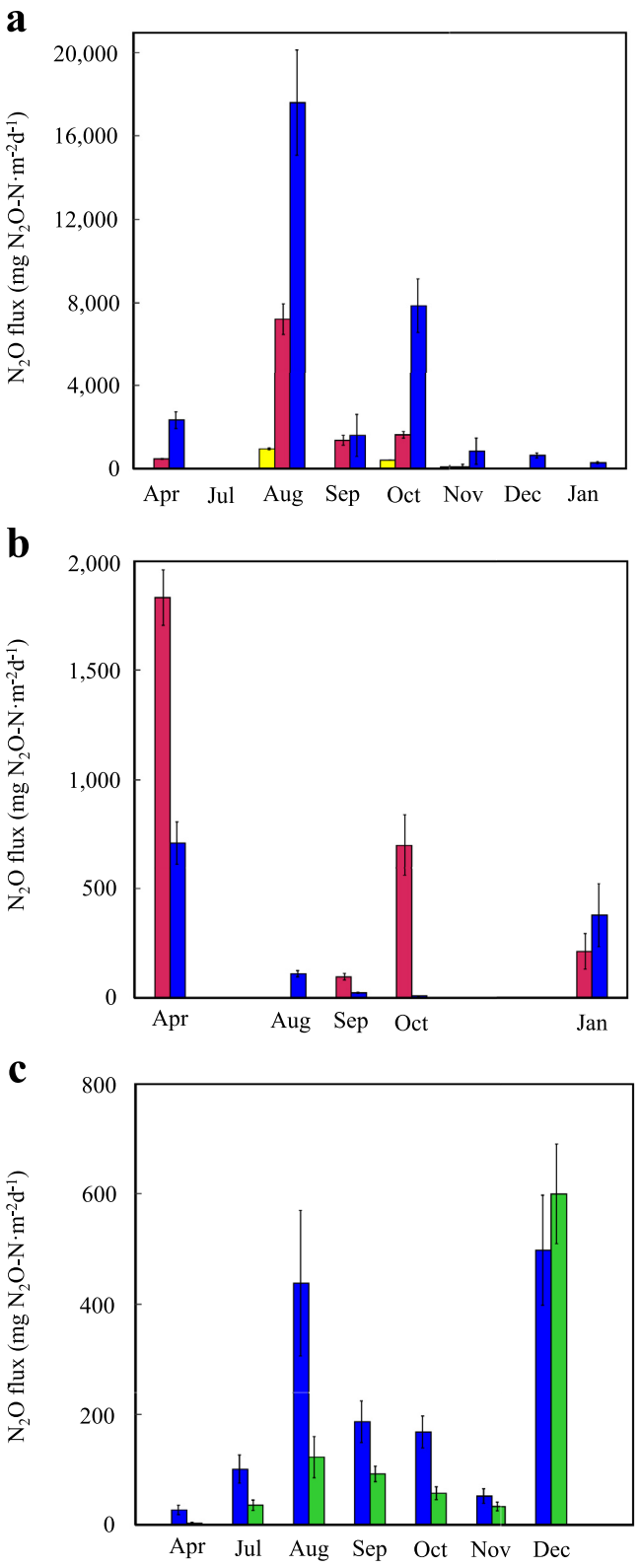

Fig. 2. The N_2O fluxes measured at the activated sludge reactors of plants A, B, and C. (a) At the plant A, the anaerobic (yellow), anoxic (red), and aerated (blue) tanks were monitered. (b) At the plant B, the anoxic (red), and aerated (blue) tanks were monitered. (c) At the plant C, the N_2O flux measurements were taken during the aeration (blue) and sedimentation (green) phases. The presented data are 30-min (a and b) or 60-min average (c) values and the error bars their standard deviations. (For interpretation of the references to colour in this figure legend, the reader is referred to the Web version of this article.)

significantly larger N_2O fluxes were measured at the aerated zone than at the anoxic zone on all eight occasions, indicating that aerobic nitrification was majorly responsible for N_2O emissions. Contrastingly, the N_2O flux was significantly higher at the anoxic zone than the aerated zone on three out of five occasions at the plant B, suggesting that contribution of denitrification to N_2O emissions was substantial at this MBR plant. The effect of temperature was ambivalent from the N_2O emissions data. More intensified N_2O emission was recorded in the warmer months (August to October) than in the colder months (April and November to January) at the plant A. Contrastingly, the largest measure of N_2O emissions were recorded in winter (December) at the plant C. No clear seasonal distinction was observed at the plant B, where the water temperature of the underground bioreactors was less affected by the outdoor air temperature. Although statistical comparisons across the WWTPs do not tell much due to the large standard deviations, both the maximum and the median values for the N_2O fluxes from both oxic and anoxic AS bioreactors were substantially higher at the plant A than at the plants B and C.

Previously, the larger N_2O emission figures often observed from the aerated AS were attributed to carryover of dissolved N_2O produced from the anoxic counterpart, as well as N_2O production from nitrification (Sun et al., 2013; Toyoda et al., 2010). The N_2O flux measurements taken at the plant B in the months of September and October suggested such carryover of N_2O was not likely. The N_2O fluxes measured at the anoxic zone were substantial (98.5 ± 15.1 mg $N_2O{-}N \cdot m^{-2} \cdot d^{-1}$ and 701.5 ± 140.2 mg $N_2O{-}N \cdot m^{-2} d^{-1}$ in September and October, respectively) during this period indicating N_2O production in the anoxic AS. The near absence of N_2O flux from the aerated tank at the same time points suggested that N_2O carryover from the anoxic zone was not a substantial contributor to N_2O emissions from the aerobic zone. The inconsistent ratio of N_2O flux from the anoxic tank to that from the aerated tank at plant A (0–0.86) also suggested insignificance of N_2O carryover from the anoxic zones to the aerated zones.

3.2. Random forest analyses and identification of key variables affecting N_2O emission from oxic and anoxic tanks

Random forest analyses were implemented to rank the nineteen variables (listed in Table S5) in accordance to their impacts on N_2O emissions from the oxic and anoxic AS of the BNR WWTPs (Fig. 3). The first round of RF analysis with the dataset obtained from the aerated AS screened out ten redundant variables with negative VIM values (temperature, pH, DO, DOC, NH_4^+-N, NO_2^--N, $DO \cdot VSS^{-1}$, $TN \cdot VSS^{-1}$, NO_2^--$N \cdot VSS^{-1}$, and NO_3^--$N \cdot VSS^{-1}$). The second round of RF analysis using the remaining nine variables identified $DIC \cdot VSS^{-1}$ and $sOUR_{AOB}$ as the most influential variables. The RF analysis with the dataset obtained from the anoxic AS identified $DOC \cdot (NO_2^-N + NO_3^-N)^{-1}$ as the most influential parameters affecting N_2O emissions, out of the four variables with positive VIM values in the first round of RF analysis. The RF classification performance was evaluated by constructing a 2×2 confusion matrix and computing the evaluation metrics (Table S6). The accuracy, sensitivity, and specificity values were 0.70, 0.75, and 0.67, respectively, for dichotomous categorization of the aerate AS datasets to high or low N_2O emissions. For anoxic AS datasets, the same calculations returned 0.77, 0.80, and 0.75, respectively. These metrics supported that the RF classifications were reliable, given the limited data size and the temporally and spatially heterogeneous nature of the WWTPs, which allowed for only limited accuracy in the measurements. The variables identified with high VIM all significantly correlated with the N_2O fluxes from the respective zones or phases of AS bioreactors (Table S7). The N_2O fluxes from the aerated AS were significantly associated with the $DIC \cdot VSS^{-1}$ ($r = 0.49$; $p =$

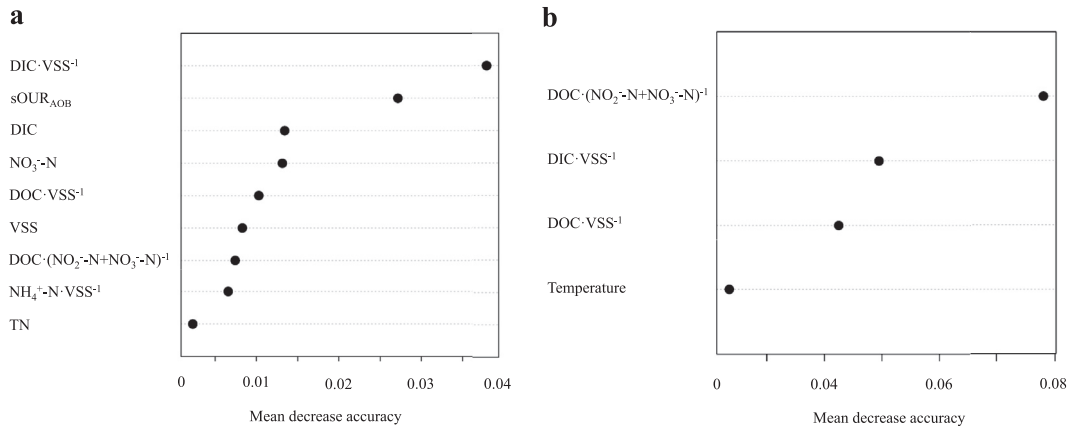

Fig. 3. Unscaled variable importance measure (VIM) values as computed from the second round of random forest analyses performed with the datasets acquired from the (a) aerated and (b) anoxic zones or phases of the examined WWTPs. Only the variables that returned positive VIM values in the first rounds of the analyses were examined. The variables were rearranged in the order of decreasing VIM values.

0.03) and $sOUR_{AOB}$ ($r = 0.47$; $p = 0.03$). Similarly, the $DOC\cdot(NO_2^-\text{-}N + NO_3^-\text{-}N)^{-1}$ values were significantly associated with N_2O fluxes ($r = -0.62$; $p = 0.02$) from the anoxic AS.

3.3. Analyses of the key variables

The two parameters identified as the most influential determinants of N_2O emissions from the aerated AS bioreactors, $DIC\cdot VSS^{-1}$ and $sOUR_{AOB}$, were significantly correlated ($r = 0.50$; $p = 0.03$), suggesting that DIC availability has significant positive impacts on NH_3 oxidation activity and N_2O production thereof (Table S7). Only a few studies have examined the relationship between DIC availability and N_2O production from nitrifying isolates or consortia and the results of these studies were largely contradictory (Jiang et al., 2015; Mellbye et al., 2016; Peng et al., 2015b). Jiang et al. (2015) and Mellbye et al. (2016) reported increased N_2O emissions at DIC-limiting conditions in axenic *Nitrosomonas europaea* cultures. The response of a complex nitrifying culture enriched from AS to varied DIC supply, as reported by Peng et al. (2015b), was contradictory to these pure culture results, in that a positive linear correlation was observed between DIC concentration and N_2O emissions within the range of DIC concentration between 4.8 and 56 mg C L^{-1}. The observations in the current study generally agrees with the latter, as the positive correlation between DIC availability and N_2O flux could be best explained with elevated N_2O-producing AOB activity at high DIC availability. The range of DIC concentrations in the aerated AS, 12.2–49.6 mg $C\cdot L^{-1}$, was sufficiently high not to cause carbon limitation to AOB, as the estimate of inorganic carbon needed for AOB growth per 1 mg $NH_4^+\cdot L^{-1}$ is 77 μg $C\cdot L^{-1}$ (van Loosdrecht et al., 2016). Nevertheless, mechanistic or physiological explanation of the observed correlations is not possible at current stage, due to the lack of information regarding the effect of excess DIC on AOB physiology.

Previously, nitrifier denitrification and heterotrophic denitrification occurring upon oxygen deficiency had been regarded as the major mechanisms of N_2O emissions from the aerated AS (Kampschreur et al., 2009; Tallec et al., 2006). That $sOUR_{AOB}$ was selected as one of the variables most influential to N_2O flux from the aerated AS and DO concentration was an insignificant parameter suggested that the majority of N_2O produced from the aerated AS bioreactors originated from biological NH_3 oxidation at oxygen-replete condition, on the contrary to the previous perception. The aerated AS bioreactors were generally maintained at high DO concentrations (the average of 4.3 ± 2.2 mg L^{-1} over all 20 measurements taken at the three facilities), and DO concentrations below 2.0 mg L^{-1} were only recorded twice (April and August) at the aerated zone of the plant B (MBR). Neither heterotrophic denitrification nor nitrifier denitrification activity was likely to be substantial at such well-oxygenated conditions (Tallec et al., 2006). Thus, the major N_2O production mechanism from the aerated AS reactors was presumably aerobic N_2O production by AOB. Although moderate in quantity as compared to nitrifier denitrification at oxygen-limited condition, AOB has been known to produce N_2O as a byproduct of NH_3 oxidation in oxygen-replete conditions (Jiang and Bakken, 1999). Several recent studies have suggested involvement of hydroxylamine (NH_2OH), the reactive intermediate of NH_3 oxidation to NO_2^-, in the oxidative N_2O production by AOB (Liu et al., 2017; Song et al., 2020). Abiotic oxidation and *n*-nitrosation, as well as incomplete oxidation of NH_2OH by hydroxylamine oxidoreductase with nitric oxide (NO) as the intermediate, have been suggested as the mechanisms of aerobic production of N_2O as a byproduct of NH_3 oxidation (Liu et al., 2017; Terada et al., 2017). N_2O emitted from the aerated AS appears to have originated from these aerobic reactions previously regarded as minor N_2O sources from nitrification.

The parameter with the largest impact to N_2O flux from the anoxic AS bioreactors of the plant A and B, according to the RF analysis, was $DOC\cdot(NO_2^-\text{-}N + NO_3^-\text{-}N)^{-1}$. The high VIM value of the parameter and its significant negative Spearman's rank correlation (Table S7; $r = -0.62$; $p = 0.02$) with the N_2O flux both supported that heterotrophic denitrification was likely the major N_2O-producing mechanism in the anoxic AS. Denitrification is carried out in multiple steps, and due to its modular nature, each step may be carried out by different guilds of organisms in a complex microbial consortia such as AS (Graf et al., 2014). In the environments with low electron donor availability, as signified by the low values of $DOC\cdot(NO_2^-\text{-}N + NO_3^-\text{-}N)^{-1}$ or more conventional C/N or COD/N ratio, limited electrons may be unevenly distributed to the different steps of denitrification (Pan et al., 2013). The intensified competition for limited electrons may result in increased N_2O production if electron donors are preferably consumed by the organismal groups responsible for the steps of denitrification upstream of N_2O. Experimental results both supporting and contradicting this hypothesis have been reported over past few decades (Itokawa et al., 2001; Kishida et al., 2004; Lu and Chandran, 2010; Pan et al., 2013). The more recent reports generally dispute against the significance of electron donor limitation to N_2O emissions, with basis on the batch kinetics of denitrifying AS consortia provided with a single

organic electron donor. For interpretation of the current result, however, dated results from less controlled reactor experiments, in which COD/N ratios turned out to be critical determinants of N_2O emissions, appear to be more applicable due to the following reasons. (1) Neither plant A nor B use organic supplements for nitrogen removal enhancement; therefore, the source of labile organic electron donor, presumably a small fraction of DOC, is of complex makeup. Different groups of denitrifiers favor different organic compounds as the sources of electrons, and thus, the kinetics of the denitrification steps in AS with complex organics may substantially differ from those observed with single organic species, e.g., methanol (Lu and Chandran, 2010; Pan et al., 2013). (2) The dissolved N_2O concentrations used in the batch kinetic assays for determination of N_2O reduction rates were orders of magnitude higher than the concentrations observed in anoxic zones of AS bioreactors (Pan et al., 2013; Wunderlin et al., 2012). As N_2O reduction follows Michaelis-Menten kinetics, the N_2O reduction rates expected *in situ* may be much lower than the linear N_2O reduction rates observed in the kinetic assays (Yoon et al., 2016).

4. Conclusion

Simultaneous monitoring of AS properties, WWTP performance, and N_2O flux at a full-scale WWTP is an onerous and time-consuming endeavor. Unless an automated monitoring system is already installed at the study site, the quantity of data obtainable from *in situ* monitoring would be always limited as relative to the number of manifold potential effecters. Not many researchers are aided with such luxury, as also was the case in this study, in which only 13–20 datasets were in hand for statistical analyses of the association between AS parameters and N_2O fluxes. Although several successful cases of fitting bench-scale reactor data or short-term (several days at the longest) to modified activated sludge models (ASM) have previously been reported, the irregularity and sheer magnitudes of fluctuations in the N_2O flux data collected in this study obviously indicated impossibility of developing a universal mathematical model estimating the N_2O emissions from full-scale AS bioreactors at different oxygen regimes (Ni et al., 2013; Spérandio et al., 2016). The approach taken here instead, the machine-learning based RF analysis, allowed for reliable binary categorization of aerated and anoxic AS conditions to high or low N_2O-emitting conditions. Besides, the WWTP parameters identified as the most influential effecters supported that the overarching microbial metabolism responsible for N_2O emissions from oxic and anoxic AS are NH_3 oxidation and denitrification, respectively.

Declaration of competing interest

The authors declare that they have no known competing financial interests or personal relationships that could have appeared to influence the work reported in this paper.

Acknowledgement

This project is supported by the "R&D Center for reduction of Non-CO_2 Greenhouse gases (2017002420002)" funded by Korea Ministry of Environment (MOE) as "Global Top Environment R&D Program".

Appendix A. Supplementary data

Supplementary data to this article can be found online at https://doi.org/10.1016/j.watres.2020.116144.

References

Aboobakar, A., Cartmell, E., Stephenson, T., Jones, M., Vale, P., Dotro, G., 2013. Nitrous oxide emissions and dissolved oxygen profiling in a full-scale nitrifying activated sludge treatment plant. Water Res. 47 (2), 524–534.
Ahn, J.H., Kim, S., Park, H., Rahm, B., Pagilla, K., Chandran, K., 2010. N_2O emissions from activated sludge processes, 2008-2009: results of a national monitoring survey in the United States. Environ. Sci. Technol. 44 (12), 4505–4511.
Apha, 2017. Standard Methods for the Examination of Water and Wastewater. American Public Health Association, Washington, DC, USA.
Breiman, L., 2001. Random forests. Mach. Learn. 45 (1), 5–32.
Chandran, K., 2011. Protocol for the measurement of nitrous oxide fluxes from biological wastewater treatment plants. Methods Enzymol. 486, 369–385.
Chandran, K., Smets, B.F., 2005. Optimizing experimental design to estimate ammonia and nitrite oxidation biokinetic parameters from batch respirograms. Water Res. 39 (20), 4969–4978.
Daelman, M.R., van Voorthuizen, E.M., van Dongen, U.G., Volcke, E.I., van Loosdrecht, M.C.M., 2015. Seasonal and diurnal variability of N_2O emissions from a full-scale municipal wastewater treatment plant. Sci. Total Environ. 536 (1), 1–11.
Díaz-Uriarte, R., Alvarez de Andrés, S., 2006. Gene selection and classification of microarray data using random forest. BMC Bioinf. 7 (1), 3.
Dodge, Y., 2008. The Concise Encyclopedia of Statistics. Springer, New York, NY, USA, pp. 502–505.
Fay, M.P., Proschan, M.A., 2010. Wilcoxon-Mann-Whitney or t-test? On assumptions for hypothesis tests and multiple interpretations of decision rules. Stat. Surv. 4, 1–39.
Flörke, M., Kynast, E., Bärlund, I., Eisner, S., Wimmer, F., Alcamo, J., 2013. Domestic and industrial water uses of the past 60 years as a mirror of socio-economic development: a global simulation study. Global Environ. Change 23 (1), 144–156.
Graf, D.R.H., Jones, C.M., Hallin, S., 2014. Intergenomic comparisons highlight modularity of the denitrification pathway and underpin the importance of community structure for N_2O emissions. PloS One 9 (12), e114118.
Gregorutti, B., Michel, B., Saint-Pierre, P., 2017. Correlation and variable importance in random forests. Stat. Comput. 27 (3), 659–678.
Hastie, T., Tibshirani, R., Friedman, J., Franklin, J., 2005. The elements of statistical learning: data mining, inference and prediction. Math. Intel. 27 (2), 83–85.
Hollister, J.W., Milstead, W.B., Kreakie, B.J., 2016. Modeling lake trophic state: a random forest approach. Ecosphere 7 (3), e01321.
IPCC, 2014. In: Edenhofer, O., Pichs-Madruga, R., Sokona, Y., Farahani, E., Kadner, S., Seyboth, K., Adler, A., Baum, I., Brunner, S., Eickemeier, P., Kriemann, B., Savolainen, J., Schlömer, S., von Stechow, C., Zwickel, T., Minx, J.C. (Eds.), Climate Change 2014: Mitigation of Climate Change. Contribution of Working Group III to the Fifth Assessment Report of the Intergovernmental Panel on Climate Change. Cambridge University Press, Cambridge, United Kingdom and New York, NY, USA, pp. 111–810.
IPCC, 2019. In: Calvo Buendia, E., Tanabe, K., Kranjc, A., Baasansuren, J., Fukuda, M., Ngarize, S., Osako, A., Pyrozhenko, Y., Shermanau, P., Federici, S. (Eds.), 2019 Refinement to the 2006 IPCC Guidelines for National Greenhouse Gas Inventories. IPCC, Switzerland, 6.61-6.62.
Itokawa, H., Hanaki, K., Matsuo, T., 2001. Nitrous oxide production in high-loading biological nitrogen removal process under low COD/N ratio condition. Water Res. 35 (3), 657–664.
Janitza, S., Strobl, C., Boulesteix, A., 2013. An AUC-based permutation variable importance measure for random forests. BMC Bioinf. 14 (1), 119.
Jiang, D., Khunjar, W.O., Wett, B., Murthy, S.N., Chandran, K., 2015. Characterizing the metabolic trade-off in *Nitrosomonas europaea* in response to changes in inorganic carbon supply. Environ. Sci. Technol. 49 (4), 2523–2531.
Jiang, Q.-Q., Bakken, L.R., 1999. Nitrous oxide production and methane oxidation by different ammonia-oxidizing bacteria. Appl. Environ. Microbiol. 65 (6), 2679–2684.
Kampschreur, M.J., Temmink, H., Kleerebezem, R., Jetten, M.S.M., van Loosdrecht, M.C.M., 2009. Nitrous oxide emission during wastewater treatment. Water Res. 43 (17), 4093–4103.
Kishida, N., Kim, J.H., Kimochi, Y., Nishimura, O., Sasaki, H., Sudo, R., 2004. Effect of C/N ratio on nitrous oxide emission from swine wastewater treatment process. Water Sci. Technol. 49 (5–6), 359–371.
Kosonen, H., Heinonen, M., Mikola, A., Haimi, H., Mulas, M., Corona, F., Vahala, R., 2016. Nitrous oxide production at a fully covered wastewater treatment plant: results of a long-term online monitoring campaign. Environ. Sci. Technol. 50 (11), 5547–5554.
Kruskal, W.H., Wallis, W.A., 1952. Use of ranks in one-criterion variance analysis. J. Am. Stat. Assoc. 47 (260), 583–621.
Krzywinski, M., Altman, N., 2015. Points of significance: multiple linear regression. Nat. Methods 12 (12), 1103–1104.
Lam, K.L., Zlatanović, L., van der Hoek, J.P., 2020. Life cycle assessment of nutrient recycling from wastewater: a critical review. Water Res. 173 (15), 115519.
Lever, J., Krzywinski, M., Altman, N., 2017. Points of significance: principal component analysis. Nat. Methods 14 (7), 641–642.
Liaw, A., Wiener, M., 2012. Package 'randomForest'. University of California, Berkeley: Berkeley, CA, USA.
Liu, S., Han, P., Hink, L., Prosser, J.I., Wagner, M., Brüggemann, N., 2017. Abiotic conversion of extracellular NH_2OH contributes to N_2O emission during

ammonia oxidation. Environ. Sci. Technol. 51 (22), 13122–13132.
Lu, H., Chandran, K., 2010. Factors promoting emissions of nitrous oxide and nitric oxide from denitrifying sequencing batch reactors operated with methanol and ethanol as electron donors. Biotechnol. Bioeng. 106 (3), 390–398.
Mellbye, B.L., Giguere, A., Chaplen, F., Bottomley, P.J., Sayavedra-Soto, L.A., 2016. Steady-state growth under inorganic carbon limitation conditions increases energy consumption for maintenance and enhances nitrous oxide production in *Nitrosomonas europaea*. Appl. Environ. Microbiol. 82 (11), 3310–3318.
Ni, B.-J., Ye, L., Law, Y., Byers, C., Yuan, Z., 2013. Mathematical modeling of nitrous oxide (N_2O) emissions from full-scale wastewater treatment plants. Environ. Sci. Technol. 47 (14), 7795–7803.
Pan, Y., Ni, B.-J., Bond, P.L., Ye, L., Yuan, Z., 2013. Electron competition among nitrogen oxides reduction during methanol-utilizing denitrification in wastewater treatment. Water Res. 47 (10), 3273–3281.
Pan, Y., Ye, L., Ni, B.-J., Yuan, Z., 2012. Effect of pH on N_2O reduction and accumulation during denitrification by methanol utilizing denitrifiers. Water Res. 46 (15), 4832–4840.
Peng, L., Ni, B.-J., Erler, D., Ye, L., Yuan, Z., 2014. The effect of dissolved oxygen on N_2O production by ammonia-oxidizing bacteria in an enriched nitrifying sludge. Water Res. 66 (1), 12–21.
Peng, L., Ni, B.-J., Ye, L., Yuan, Z., 2015a. The combined effect of dissolved oxygen and nitrite on N_2O production by ammonia oxidizing bacteria in an enriched nitrifying sludge. Water Res. 73 (15), 29–36.
Peng, L., Ni, B.-J., Ye, L., Yuan, Z., 2015b. N_2O production by ammonia oxidizing bacteria in an enriched nitrifying sludge linearly depends on inorganic carbon concentration. Water Res. 74 (1), 58–66.
Powers, D.M., 2011. Evaluation: from precision, recall and F-measure to ROC, informedness, markedness and correlation. J. Mach. Learn. Res. 2 (1), 37–63.
Rodríguez-Caballero, A., Aymerich, I., Marques, R., Poch, M., Pijuan, M., 2015. Minimizing N_2O emissions and carbon footprint on a full-scale activated sludge sequencing batch reactor. Water Res. 71 (15), 1–10.
RStudio Team, 2015. RStudio: Integrated Development for R. RStudio, Inc., Boston, MA. http://www.rstudio.com/.
Song, M.J., Yoon, H., Lee, T.-K., Kwon, M., Yoon, S., 2020. Orthophosphate enhances N_2O production from aerobic hydroxylamine decomposition: implications to N_2O emissions from nitrification in ornithogenic and manure-fertilized soils. Biol. Fertil. Soils 56, 687–695.
Spérandio, M., Pocquet, M., Guo, L., Ni, B., Vanrolleghem, P.A., Yuan, Z., 2016. Evaluation of different nitrous oxide production models with four continuous long-term wastewater treatment process data series. Bioproc. Biosyst. Eng. 39 (3), 493–510.
Statnikov, A., Wang, L., Aliferis, C.F., 2008. A comprehensive comparison of random forests and support vector machines for microarray-based cancer classification. BMC Bioinf. 9 (1), 319.
Strobl, C., Boulesteix, A., Zeileis, A., Hothorn, T., 2007. Bias in random forest variable importance measures: illustrations, sources and a solution. BMC Bioinf. 8 (1), 25.
Sun, S., Cheng, X., Li, S., Qi, F., Liu, Y., Sun, D., 2013. N_2O emission from full-scale urban wastewater treatment plants: a comparison between A2O and SBR. Water Sci. Technol. 67 (9), 1887–1893.
Tallec, G., Garnier, J., Billen, G., Gousailles, M., 2006. Nitrous oxide emissions from secondary activated sludge in nitrifying conditions of urban wastewater treatment plants: effect of oxygenation level. Water Res. 40 (15), 2972–2980.
Tang, J., Alelyani, S., Liu, H., 2014. Feature selection for classification: a review. In: Data Classification: Algorithms and Applications. CRC Press, pp. 37–64.
Terada, A., Sugawara, S., Hojo, K., Takeuchi, Y., Riya, S., Harper, W.F., Yamamoto, T., Kuroiwa, M., Isobe, K., Katsuyama, C., Suwa, Y., Koba, K., Hosomi, M., 2017. Hybrid nitrous oxide production from a partial nitrifying bioreactor: hydroxylamine interactions with nitrite. Environ. Sci. Technol. 51 (5), 2748–2756.
Toyoda, S., Suzuki, Y., Hattori, S., Yamada, K., Fujii, A., Yoshida, N., Kouno, R., Murayama, K., Shiomi, H., 2010. Isotopomer analysis of production and consumption mechanisms of N_2O and CH_4 in an advanced wastewater treatment system. Environ. Sci. Technol. 45 (3), 917–922.
van de Graaf, A.A., de Bruijn, P., Robertson, L.A., Jetten, M.S., Kuenen, J.G., 1996. Autotrophic growth of anaerobic ammonium-oxidizing micro-organisms in a fluidized bed reactor. Microbiology 142 (8), 2187–2196.
van Loosdrecht, M.C.M., Nielsen, P.H., Lopez-Vazquez, C.M., Brdjanovic, D., 2016. Experimental Methods in Wastewater Treatment. IWA publishing, London, pp. 73–76.
Vasilaki, V., Massara, T., Stanchev, P., Fatone, F., Katsou, E., 2019. A decade of nitrous oxide (N_2O) monitoring in full-scale wastewater treatment processes: a critical review. Water Res. 161 (15), 392–412.
Vasilaki, V., Volcke, E.I.P., Nandi, A.K., van Loosdrecht, M.C.M., Katsou, E., 2018. Relating N_2O emissions during biological nitrogen removal with operating conditions using multivariate statistical techniques. Water Res. 140 (1), 387–402.
Vieira, A., Galinha, C., Oehmen, A., Carvalho, G., 2019. The link between nitrous oxide emissions, microbial community profile and function from three full-scale WWTPs. Sci. Total Environ. 651 (15), 2460–2472.
Vincenzi, S., Zucchetta, M., Franzoi, P., Pellizzato, M., Pranovi, F., De Leo, G.A., Torricelli, P., 2011. Application of a Random Forest algorithm to predict spatial distribution of the potential yield of *Ruditapes philippinarum* in the Venice lagoon. Italy. Ecol. Model. 222 (8), 1471–1478.
Wunderlin, P., Mohn, J., Joss, A., Emmenegger, L., Siegrist, H., 2012. Mechanisms of N_2O production in biological wastewater treatment under nitrifying and denitrifying conditions. Water Res. 46 (4), 1027–1037.
Yoon, S., Nissen, S., Park, D., Sanford, R.A., Löffler, F.E., 2016. Nitrous oxide reduction kinetics distinguish bacteria harboring clade I versus clade II NosZ. Appl. Environ. Microbiol. 82 (13), 3793–3800.